J Mater Sci: Mater Electron **(2023) 34:1995**

The role of cordierite nano filler on the electrical, mechanical, thermal, and chemical properties of liquid silicone rubber used in composite insulators

Shirisha Adupa[1,*], Chennakesava Reddy Alavala[2], and Sammaiah Pulla[3]

[1] *Department of Mechanical Engineering, Jawahralal Nehru Technological University, Hyderabad, India*
[2] *Mechanical Engineering Department, Jawahralal Nehru Technological University, Hyderabad, India*
[3] *Department of Mechanical Engineering, S R University, Warangal, India*

Received: 7 March 2023
Accepted: 2 October 2023
Published online: 15 October 2023

ABSTRACT

In this research cordierite ($2MgO\ 2Al_2O_3\ 5SiO_2$)/liquid silicone rubber (LSR) blends were synthesized by adding the cordierite nano filler with varying weight percentages (5, 10, 15) to LSR. Mechanical, thermal, electrical, structural, physical, and chemical properties were investigated for different blend samples and compared to pure LSR. The findings suggest that incorporating cordierite into liquid silicone rubber improved hardness, density, and electrical properties such as dielectric constant, DC volume resistivity, arc resistance, hydrophobicity, and dielectric breakdown strength, which are appealing in the realm of insulating materials for outdoor insulation applications, particularly in the field of transmission and distribution lines.

1 Introduction

Cordierite ceramic is a magnesium aluminum silicate material with the general formula $2MgO.\ 2Al_2O_3.\ 5SiO_2$. (Al_2O_3, SiO_2, and MgO are the high surface area inorganic fillers corresponding to an oxide composition of 51.3% SiO_2, 34.9% Al_2O_3, and 13.8% MgO) [1–3]. Cordierite ceramics are hi-tech ceramic materials having low thermal expansion coefficients, good high-temperature performances than alumina [4], strong dielectric properties than aluminium nitride, silicon nitrides, high specific surface areas, and good adsorption capabilities. These benefits have led to cordierite ceramics being used in high-tech industries like bio-ceramics, low-temperature heat radiation, and electronic packaging. It has been widely employed in applications requiring thermal shock resistance [5].

High insulation levels and dependable physical and chemical properties are well-known characteristics of polymers. In comparison to most organic polymers, silicone rubber performed better in applications for outdoor insulators. Nonetheless, polymer composites outperform basic polymers in a variety of ways [6]. Polymer nano composites (which are formed of nanoscale sized fillers that are homogeneously disturbed throughout the polymer matrix) have received

Address correspondence to E-mail: adupashirisha@gmail.com

https://doi.org/10.1007/s10854-023-11421-7

a lot of interest in recent years due to their better stability, longer lifespan, and superior physical, electrical, optical, and mechanical capabilities. Since the 1960's, when they first debuted on the market, composite insulators have gained enormous popularity among utilities and equipment manufacturers all over the world. Composite designs are preferable to ceramic insulators because they are lighter in weight, less likely to break, function better during earthquakes, and allow for more design flexibility. The possible outcomes of these features are reduced installation costs, increased durability, and more aesthetically beautiful line design. In light of its exceptional qualities, analysis of the available data has revealed that polymer nano composite has promise as a near-term enhanced dielectric and electrical insulation [7].

The following qualities should meet the performance requirements of outdoor insulation materials: (1) High insulation resistance to prevent leakage current. (2) To avoid electrical breakdown, dielectric strength should be high. (3) High mechanical strength is required to withstand the handling by mechanical means. (4) Lowest thermal conductivity should be a requirement for the best insulation materials [8].

For polymeric dielectric composites in the past, two different approaches were used.

1) In the first approach, conductive fillers were added to the polymer network to create a percolating system. This strategy is based on the findings that a crucial filler volume might result in a very high permittivity. However, despite the low dielectric constant, a substantial dielectric loss was recorded in this scenario.
2) The second approach was developed by incorporating ceramic insulating fillers. This technique might produce satisfactory results, however depending on size, greater filler loadings are needed, which sacrifice fundamental qualities like mechanical strength and flexibility.

Moreover, in any approach, the uniform dispersion of fillers is essential for attaining the desired characteristics [9].

In this paper, we concentrated on composite polymeric materials such as LSR/cordierite nano composites for electrical insulation applications as well as we used the above discussed second approach, and the results were consistent with the assertion provided in the relevant approach. When compared to pure LSR, it was found that the addition of nano cordierite particles improved the electrical properties such as dielectric constant (11%), DC volume resistivity (2%), arc resistance (660%), and dielectric breakdown strength (32%), but slightly decreased the mechanical properties such as tensile strength (20%), tear strength (7%), and elongation at break (17%).

The LSR/cordierite nano composite's obtained mechanical strength was superior to that of LSR/35wt% TiO_2, SR/1.0vol% BN, SR/0.7wt% functionalized grapheme and elongation at break was superior to that of PMVQ/2phr CeO_2/0.8phr Graphene, SR/5wt%ZnO, SR/5wt%SiO_2, LSR/35wt% TiO_2, ATH-SIR, SR/40phr fumed silica, SR/0.7wt% functionalized grapheme [8].

LSR/cordierite nano composites showed better dielectric constant than SR/5wt%TiO_2, SR/12wt%BN, ATH-SIR, SIR/Alumina, SIR/Titania, SR/micro–Si_3N_4/nano–Al_2O_3, and a greater breakdown strength than LSR/10wt%Al_2O_3 [8]. The thermal conductivity of LSR/cordierite nano composites was better than that of SR/micro–Si_3N_4/nano–Al_2O_3, SR/14% BN nanoplates, SR/ABN150 (Aligned Boron Nitride), ATH-SIR, and SR/ZnOw/m-ZnOs [8].

According to the aforementioned findings, it is applicable to the industries of electronics, aviation, aerospace, bake ware, cookware, cable accessories, automotive, medical devices, veterinary medicine, moulding, and semi-conductors [8].

2 Materials and methods

2.1 Materials

The liquid silicone rubber (Siloczest LSR-3) employed as the matrix in this investigation was supplied by Chemzest Technoproducts Pvt Ltd, Chennai, India. This silicone rubber is a two-part silicone with a specific gravity of 1.18 that is intended for usage with a platinum catalyst mix ratio of 100:10. Chemzest Technoproducts Pvt Ltd, Chennai, India, supplies the mould release agent, which is manufactured by Aerol Formulations Pvt. Ltd., New Delhi, India. The cordierite ($2MgO\ 2Al_2O_3\ 5SiO_2$) nanoparticles had a purity of 99.5%, a density of 2.1-2.6gm/cc, and an average particle size of 40 nm. They were acquired from the Nano Research Lab in Jharkhand, India.

2.2 Sample preparation

In this study, composite samples with varying filler loadings were created using the cast moulding procedure. All of the LSR, cordierite filler, and catalyst were meticulously weighed to three decimal places. The composites were then mechanically agitated for 50 min at room temperature at a speed of 2100 rpm. The catalyst was then completely mixed with the binder before being placed in a vacuum degassing chamber for 5 to 10 min, or until all air bubbles were dispersed. We put the composite binder into the mould after spraying the mould release agent and allowed it to cure at room temperature.

2.3 Characterization

The FE-SEM images of the LSR-cordierite composite samples with dimensions of 1 × 1 cm^2 are characterized by the Zeiss Gemini FE-SEM (model) from Carl Zeiss(make). The XRD patterns of the cordierite samples with dimensions of 1 × 1cm^2 are analyzed by a XPert powder PANalytical X-ray diffractometer model 7602 EA ALMELO (The Netherlands). Tensile, tear, and hardness tests were used to measure the mechanical properties of LSR composite samples. The selected dimensions of 150 mm × 150 mm × 3 mm, 150 mm × 150 mm × 4 mm, and 150 mm × 150 mm × 5 mm samples were prepared and cut into specific sizes of dumbbell shape shown in below Fig. 1a for mechanical tension testing according to ASTM D 412, and specific dimensions for tear testing shown in Fig. 1 according to ASTM D 624. Tensile and tear tests were performed using a DTRX 30KN universal testing equipment in line with the DPPL/13-14/01191-1264533 standard test protocol for elastomers. At room temperature, the measurements were collected with a 50 kg load sensor. Two samples from each mix were measured at the same elongation rate. In accordance with ASTM D 2240 guidelines, the hardness measurements were performed using an Eco-SR shore A hardness durometer (model number 2120) shown in below Fig. 1b along with the sample to be tested. Dielectric constant, DC volume resistivity, Break down strength (dielectric strength), and Arc resistance tests were used to investigate the electrical properties of LSR composite samples. Dielectric constant is measured for few rectangular shaped samples of 3 mm thickness prepared from each composition using DIELECTRIC CONSTANT METER (KL/DCM/01, Sivananda electronics, India) and disc shaped samples of 50 mm diameter and 3 mm thickness prepared from each composition and tested for its Arc resistance based on ASTM D 495 using ARC RESISTANCE TEST Equipment and the test sample is shown in Fig. 2a below. Rectangular samples of 100 mm × 100 mm × 2 mm were prepared from each composition and tested for DC volume resistivity using DIGITAL MILLION MEGOHM METER (LS-3CD, Sivananda Electronics, India) as per IEC 60,093 shown in Fig. 2b, dielectric breakdown voltage based on ASTM D 149 using H.V. BREAK DOWN TESTER (South Eastern Equipment CO., India), and hydrophobicity recovery as per IEC 61109 and the tested samples are shown in Fig. 2c. Thermal conductivities of disc-shaped samples shown in Fig. 3 of 50 mm diameter and 3 mm thickness from each composition were evaluated using an ASTM E 1530-compliant thermal conductivity tester (Anter corporation USA 2008). The weight loss of the LSR-Cordierite composites was measured using a thermo gravimetric analyzer (model: SII 6300 EXSTAR) in an air environment ranging from 35 to 300 °C at a heating rate of 10 °C/min. To assess the physical characteristic, square samples

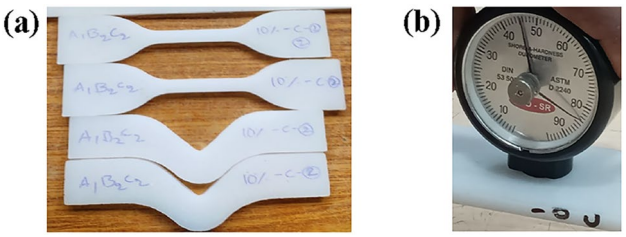

Fig. 1 **a** Tensile and tear test samples, **b** shore A hardness testing

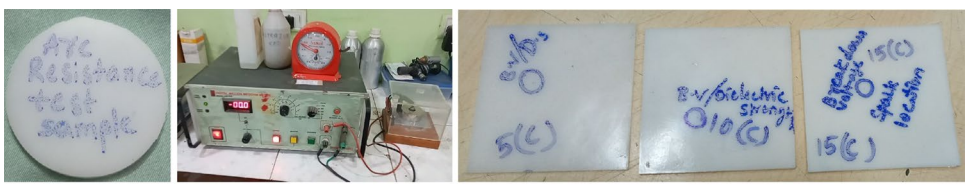

Fig. 2 **a** Arc resistance test sample, **b** DC volume resistivity test, **c** break down voltage, DC volume resistivity, hydrophobicity test samples.

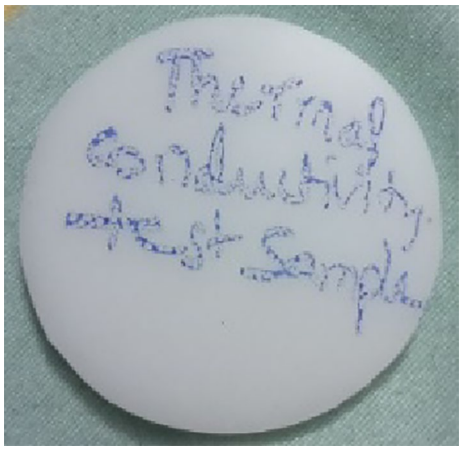

Fig. 3 Thermal conductivity test sample

Fig. 4 Specific gravity test setup

with dimensions of 10 mm × 10 mm were utilised for the specific gravity test based on ASTM D 792 shown in below Fig. 4. The same dimensional samples were used to perform chemical characteristics such as corrosion resistance shown below in Fig. 5.

2.4 Experimental design for mechanical testing samples

The experimental design for testing samples for mechanical properties is based on Taguchi's L9 orthogonal array. The design process parameters are described in Table 1 in detail. Table 2 provides information about the experiment design.

Fig. 5 Immersion of samples in chemical solutions

Table 1 process parameters used in the design of experiment

A (% of reinforcement in LSR)	B (sample thickness)	C (curing time)
A_1 (5%)	B_1 (3 mm)	C_1 (24 h)
A_2 (10%)	B_2 (4 mm)	C_2 (36 h)
A_3 (15%)	B_3 (5 mm)	C_3 (48 h)

Table 2 Experimental design based on Taguchi's L9 orthogonal array

Experiment No	Parameter A in %	Parameter B in mm	Parameter C in hours (hrs)
1	5	3	24
2	5	4	36
3	5	5	48
4	10	3	36
5	10	4	48
6	10	5	24
7	15	3	48
8	15	4	24
9	15	5	36

3 Results and discussions

3.1 Structural characterization

The main objective of structural characterization of nanomaterials is to investigate the structure-property relationship and identify novel properties in order to make meaningful advancements in the revolutionary materials currently available. The characterisation of nanomaterials is an important research technique for raising the effectiveness of production procedures. Nanomaterials with sizes ranging from a few

nanometers to 500 nm have been discovered using various characterization techniques such as SEM, TEM, and XRD.

3.1.1 FE-SEM surface morphological studies

The microstructure of the materials can be visualised using field emission scanning electron microscopy (FE-SEM), a cutting-edge technique. Gas molecules have a tendency to interfere with the electron beam and the secondary and backscattered electrons that are generated, which are utilised for imaging, hence FE-SEM is normally carried out in a high vacuum. FE-SEM surface morphological studies of Cordierite/LSR composites are shown in Fig. 6. Filler reinforcement has a significant impact on many properties of a polymeric composite material, particularly in the case of rubber. Fletcher and Gent provide an explanation of the filler-rubber interaction, and Payne further improves the investigation. Yasin also talked about how ionic liquids can be used to disperse filler. Basically, the primary variables that affect the actual contact area between the rubber and filler are the particle sizes, the amount of loading, and the specific surface area. Rubber and filler may interact physically or chemically in this way [9]. This interaction is chemical in the cordierite and LSR scenario.

3.1.2 XRD

Figure 7 displays the XRD patterns of pure LSR and composites loaded with cordierite. We can see from the XRD patterns of pure LSR there is no crystalline phase present in these residues; only amorphous humps are seen [10]. According to the XRD patterns of nano cordierite filled LSR composites, the miller planes of cordierite that the detected diffraction peaks of 2Θ at 21.63°, 26.38°, 28.37°, 29.58°, 30.8°, 33.75°, 36.5°, 38.45°, 43.12°, 44.3°, 58.9°, and 64.9° referred to were 102, 112, 202, 211, 220, 212, 311, 310, 312, 400, 511, and 440 respectively. The sample's crystalline phase has been identified as α-cordierite (JCPDS card no. 84-1222) [11, 12].

3.2 Mechanical and physical properties

Table 3 displays the findings of various mechanical properties of cordierite-filled and pure LSR composites.

3.2.1 Tensile strength

The tensile strength of LSR composites varied depending on sample thickness and filler loading, as shown in Fig. 8. Tensile strength values for 3 mm thick LSR composites climb from 2.775 to 3.185 Mpa when filler loading increases from 5 to 15% weight and curing duration increases from 24 to 48 h. These findings suggest that greater the filler loading and curing period, the greater the tensile strength for the same thickness sample.

The plot shows that the tensile strengths of the 5 mm thick composite samples increased from 2.615 to 2.995 Mpa from 5 to 10 wt% and decreased from 2.995 to 2.875 Mpa from 10 to 15 wt%. Figure 6 FE-SEM surface morphological studies shows that in a 10 wt% composite sample, there is a continuous and uniform distribution of MgO and Al_2O_3 particles, however in a 15 wt% composite sample, there is a discontinuity in MgO and Al_2O_3, resulting in a drop in tensile strength. Another finding is that tensile strength decreases with increasing filler loading and curing time. Tensile strength readings of 4 mm thick samples at any filler loading followed the plot's almost consistent trend. From Table 3 it is observed that the results of tensile strengths of all these LSR composite samples are seen to decline when compared to pure LSR as 3.98 Mpa.

The cordierite filled LSR composite sample with a thickness of 3 mm, a filler loading of 15 wt%, and a curing duration of 48 h had the highest tensile strength of 3.185 MPa of all composite samples. This is because the particle concentration in 3 mm samples is higher due to the smaller cross sectional area compared to 4 and 5 mm thick samples, hence tensile strength improves.

3.2.2 Tear strength

The tear strength of LSR composites varied depending on sample thickness and filler loading, as shown in Fig. 9. Tear strength values for 3 mm thick LSR composites improve from 12.73 to 15.65 N/mm when filler loading increases from 5 to 15 wt% and curing duration increases from 24 to 48 h. These findings demonstrate that the higher the filler loading and curing period, the greater the tear strength for the same thickness sample.

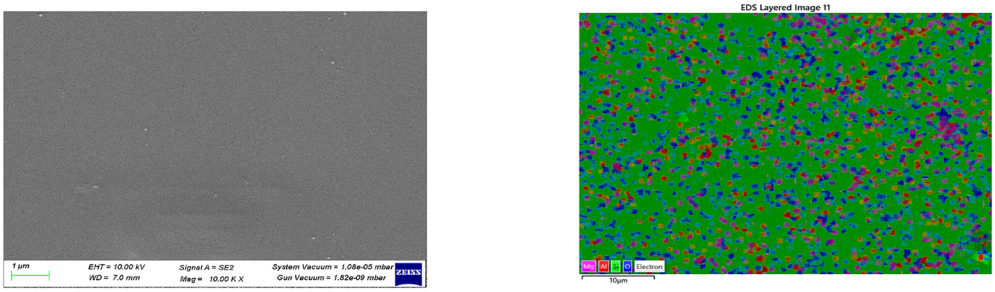

a) LSR with 5% cordierite 4mm thick (sample 2)

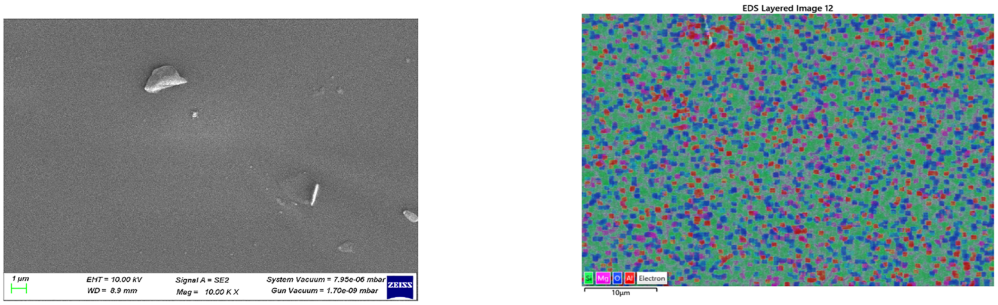

b) LSR with 10% cordierite 4mm thick (sample 5)

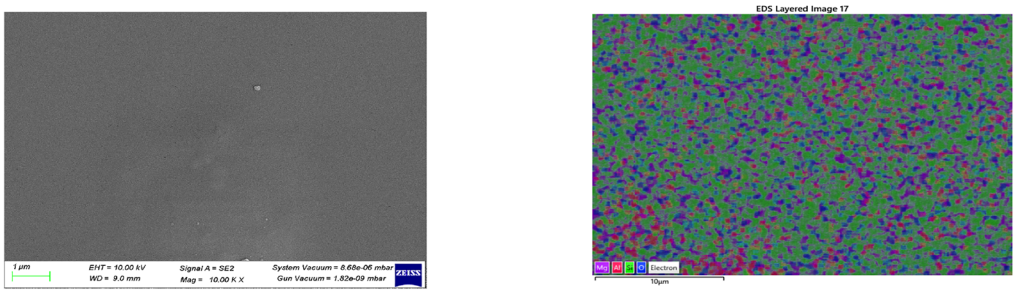

c) LSR with 15% cordierite 4mm thick (sample 8)

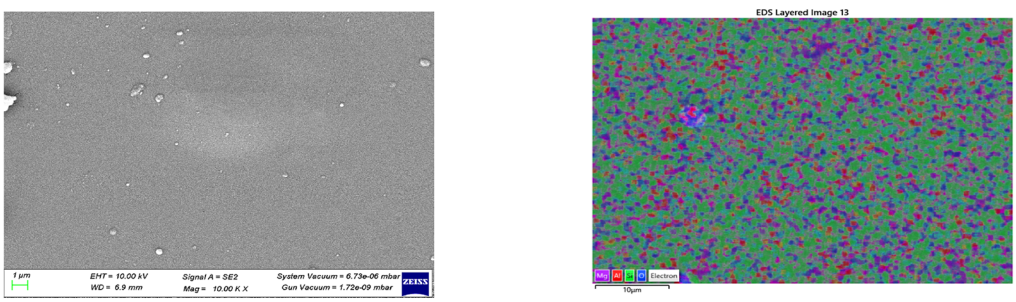

d) LSR with 10% cordierite 5mm thick (sample 6)

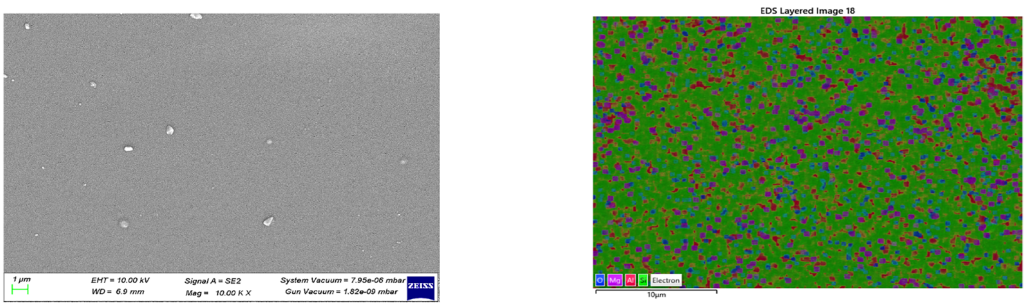

e) LSR with 15% cordierite 5mm thick (sample 9)

◂**Fig. 6** FE-SEM surface morphological studies of cordierite filled LSR composites

The tensile strengths of the 4 mm thick composite samples increased from 16.08 to 17.74 N/mm from 5 to 10 wt% and decreased from 17.74 to 9.29 N/mm from 10 to 15 wt%. Another observation is that when filler loading and curing time increase, tear strength falls. 5 mm thick samples exhibit the same trend as 4 mm thick samples, however rip strength diminishes with increasing filler loading and curing time. Only a 5 mm thick, 10 wt% filler load, and 24 h cured cordierite filled LSR composite sample demonstrated the highest tear strength of 19.04 N/mm among all composite samples, excluding pure LSR, which was 20.16 N/mm. The Fig. 6 FE-SEM surface morphological studies revealed a similar pattern for all samples, as mentioned in the Tensile strength section.

3.2.3 Elongation at break

The elongation at break value for pure LSR is 416.06%, but cordierite infused LSR composites result in a significant drop to just 270% for the 3 mm thick, 48 h cured, 15 wt% sample. The average values of percentage elongation at break obtained from Table 3 mentioned values fell from 337 to 290% for all created blends with the inclusion of cordierite nano particles in varied weight percentages from 5 to 15 wt%. According to shore hardness data, the decrease in % elongation at break indicates that the stiffness of the filler begins to dominate the property as cordierite concentration increases, which can diminish the elongation at break of LSR composites. Furthermore, as seen in Fig. 10, the samples' decreasing behaviour was nonlinear.

The largest % elongation values were 336.39% for the 3 mm thickness sample that was cured in 24 h, 343.74% for the 4 mm thickness sample that was cured in 36 h, and 335.35% for the 5 mm thickness sample that was cured in 24 h.

This leads us to the conclusion that the highest % elongation at break values were obtained from each thickness composite sample; as the thickness grows from 3 to 5 mm, the curing time first goes from minimum to moderate (24 to 36 h) and then returns to minimal. The Fig. 6 FE-SEM surface morphological studies showed a consistent trend for all samples, which is similar to the pattern seen in the Tensile strength section.

3.2.4 Shore a hardness and density

The Fig. 11 depicts the shore A hardness and density of the samples. The Shore hardness of pure LSR is 42.5. The hardness increased consistently as the cordierite nano filler percentage increased, from 44.5 for a 5 wt% cordierite sample to 48 for a 15 wt% cordierite sample. This enhancement is attributed to particles size, uniform dispersion, higher molecular interactions, and improved cross-linking among particles and base matrix [13]. Cordierite is undoubtedly hard filler. Many other polymer composites have shown an increase in hardness with increasing concentrations of inorganic fillers [14].

Based on the Archimedes approach, the sample densities were determined. The measured density of the pure and cordierite-filled LSR samples is shown in Fig. 11, increasing from 1.0381 g/cc for the empty LSR to 1.1603 g/cc for the 15 wt% cordierite-filled sample. The findings showed that, because cordierite filler density is higher than that of LSR density, the densities of composite samples rose as the filler loading increased [15].

3.3 Electrical properties

The results of various electrical characteristics of pure LSR and cordierite loaded LSR composites are shown in Table 4.

3.3.1 Dielectric constant and dielectric breakdown strength

Material's degree of polarization in the presence of an electric field is described by a dielectric constant. Combining ionic, electronic, and interfacial polarisation led to the determination of dielectric constants. Dielectric constant requirements vary depending on the application sector. An insulating medium requires a lower dielectric constant than a substance used as a capacitor, which requires a higher dielectric constant. The dielectric constant of a composite is influenced by the polymer matrix, particles, and the interface region created by them [16]. The capacitance of each sample was measured first in this test, and the formula for computing the dielectric constant is given by.

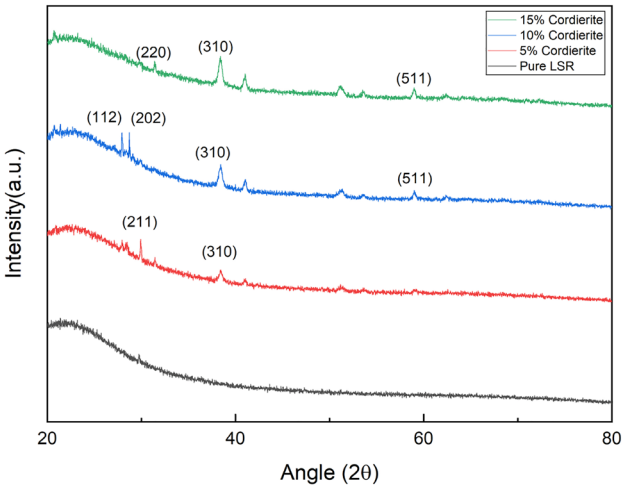

Fig. 7 XRD patterns of pure LSR and cordierite filled LSR composites

$$D_s = 0.57521 \times C_x \times t,$$

where D_s is the dielectric constant, C_x is the capacitance, t is the thickness of the sample. At 1 MHz frequency, Fig. 12 displays the change in dielectric constant of LSR and its composites. The dielectric constant values for 5 wt% and 15 wt% cordierite filled LSR composite samples were 3.14 and 3.38, respectively, which are lower than the dielectric constant value for pure LSR, which was 3.5119. A 10 wt% cordierite filled LSR composite with an enhanced dielectric constant value of 3.74 was measured, indicating that this composite has slightly higher charge-storing ability than the rest samples. These increased dielectric constant values of pure LSR and 10 wt% filled LSR composites are caused by polar groups that line up with the applied electric field. Furthermore, it takes an unlimited amount of time for the charge carriers to align themselves. Typically, polymeric materials have a large dielectric constant at low frequencies, but it drops with frequency and eventually reaches a constant value [9].

The dielectric breakdown strength is computed by dividing the breakdown voltage by the sample thickness and is represented in kV/mm. Figure 12 depicts the increase in composite dielectric breakdown strength ratings attained in this investigation by varying the weight percentages of cordierite fillers added to liquid silicone rubber. As the filler loading increases, so do the dielectric breakdown strength values. The dielectric breakdown strength for 5% cordierite by weight was determined to be 11.95 kV/mm, which is 27% less than the breakdown strength figure for pure LSR, which is 16.45 kV/mm. According to the Fig. 6 FE-SEM surface morphological studies images, the decrease in the breakdown strength of nano composites induced by uneven dispersion of ceramic nano particles increases the intensity of the local electric field, which improves the dielectric response slightly [17]. The dielectric breakdown strength was determined to be 17.56 kV/mm for a filling amount of 10% cordierite by weight, which is 7% greater than the breakdown strength value of pure LSR. For a filling amount of 15% cordierite by weight, the maximum dielectric breakdown strength was determined to be 21.72 kV/mm, which is 32% higher than the breakdown strength value for pure LSR. The increased dielectric breakdown strength of the composites is generated by mobile charge carriers being trapped in the contact region between the polymer matrix and the ceramic reinforcement, which limits the establishment of electrical conduction channels. Another cause was the

Table 3 Mechanical property experimental findings

Sample number	Sample name	Sample code	Tensile strength in MPa (ASTM D 412)	Tear strength in N/mm (ASTM D 624)	Elongation at break in %
1	Pure LSR	–	3.98	20.615	416.06
2	LSR with 5% cordierite	$A_1B_1C_1$	2.775	12.73	336.39
3	LSR with 5% cordierite	$A_1B_2C_2$	2.805	16.085	343.74
4	LSR with 5% cordierite	$A_1B_3C_3$	2.615	15.538	334.96
5	LSR with 10% cordierite	$A_2B_1C_2$	2.975	13.188	319.82
6	LSR with 10% cordierite	$A_2B_2C_3$	2.75	17.743	303.15
7	LSR with 10% cordierite	$A_2B_3C_1$	2.995	19.045	335.35
8	LSR with 15% cordierite	$A_3B_1C_3$	3.185	15.655	270.07
9	LSR with 15% cordierite	$A_3B_2C_1$	2.795	9.291	308.39
10	LSR with 15% cordierite	$A_3B_3C_2$	2.875	11.679	292.09

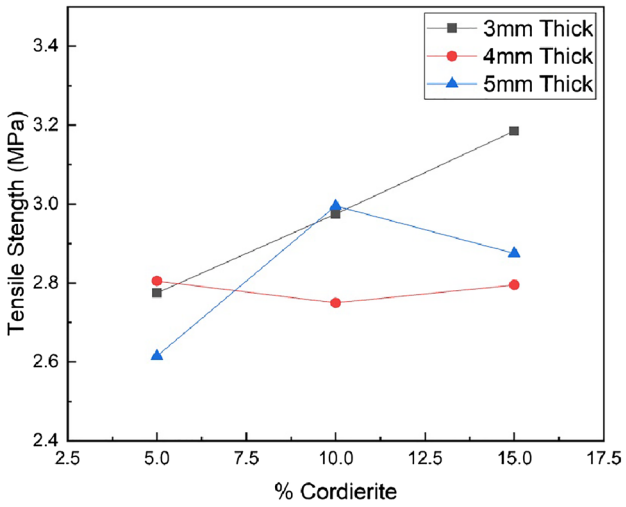

Fig. 8 Tensile strengths of LSR composites with different loadings of cordierite

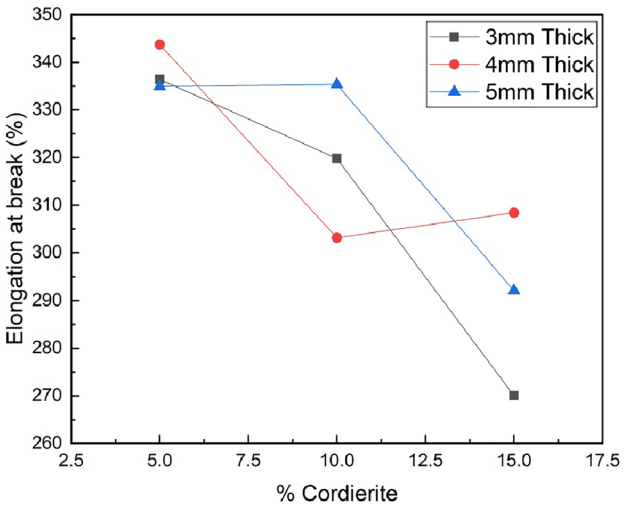

Fig. 10 Elongation at break of LSR composites with different loadings of cordierite

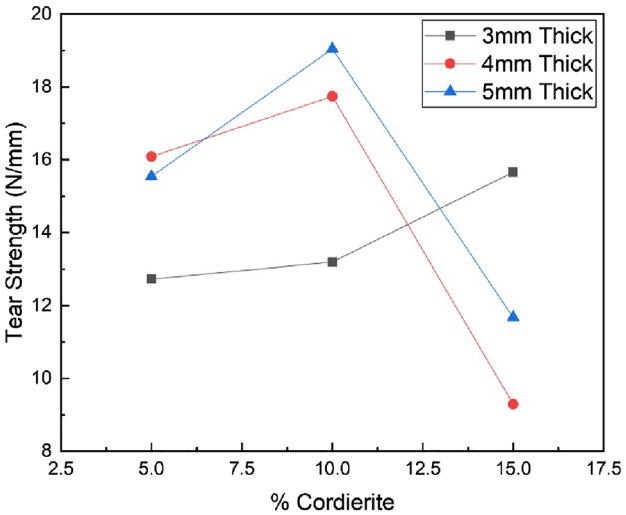

Fig. 9 Tear strengths of LSR composites with different loadings of cordierite

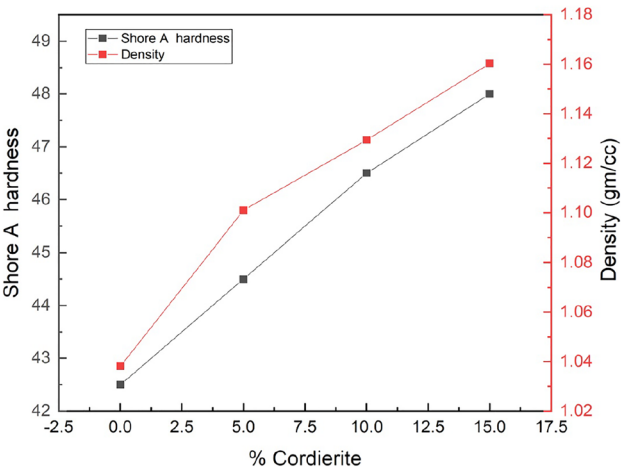

Fig. 11 Shore A hardness and density of pure and cordierite filled LSR composites

decreased surface energy, filler dispersion in the polymer matrix, improved hydrophobicity, and the bonding forces of the Si–O link. Furthermore, the rise in heat conductivity after loading ceramic filler is another element for boosting composite dielectric strength [18–20].

3.3.2 *DC volume resistivity and arc resistance test*

Volume resistivity is an essential consideration when picking a material for electrical insulation applications since it functions as a barrier to leaking current thru out the body of a dielectric substance. The volume resistivity increases as the leakage current decreases and the material becomes less conductive. In Fig. 13, the volume resistivity of pure LSR and LSR/cordierite composites at the 250 V DC field is depicted. The volume resistivity of 0 wt%, 5 wt%, 10 wt%, 15wt % cordierite/LSR composites is 8.6265×10^{16}, 8.6469×10^{16}, 8.7796×10^{16}, 8.7898×10^{16} Ω cm respectively. The well-known industry formula for volume resistivity is equals $A \times R/t$, where A is the area of the test jig plates, R defines resistance, and t denotes material thickness. According to the findings, filler

Table 4 Experimental results of electrical properties

Sample name	Dielectric constant (ASTM D 150)	DC Volume resistivity in ohm cm (IEC 60,093)	Dielectric breakdown strength in kv/mm (ASTM D 149)	Arc Resistance in seconds (ASTM D 495)
Pure LSR	3.5119	8.6265×10^{16}	16.45	23
LSR with 5% cordierite	3.14	8.6469×10^{16}	11.95	175
LSR with 10% cordierite	3.74	8.7796×10^{16}	17.56	124
LSR with 15% cordierite	3.38	8.7898×10^{16}	21.72	145

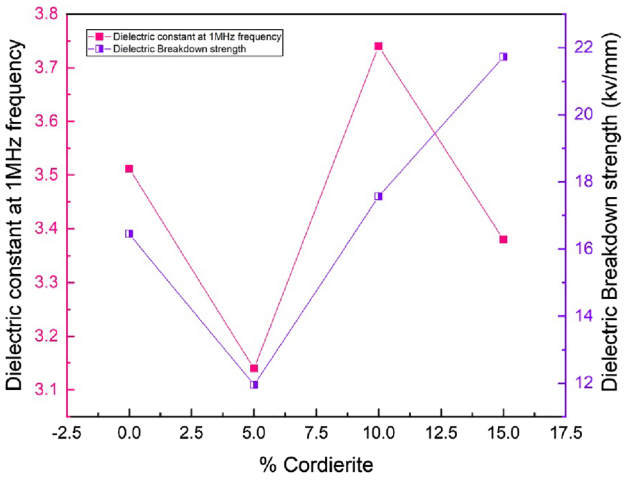

Fig. 12 Dielectric constant at 1 MHz frequency and dielectric breakdown strength of LSR composites with different loadings of cordierite

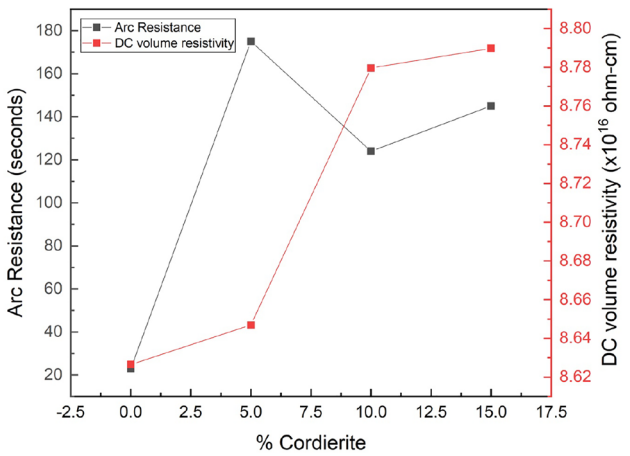

Fig. 13 DC volume resistivity and arc resistance test values for Cordierite filled LSR composites

deposition increases the volume resistivity of the LSR. As per earlier studies, adding MgO, ZnO, and Al_2O_3 nanoparticles would create a large number of deep traps at the interfaces between the nanoparticles and the polymer matrix. These deep traps might trap charge carriers, lower their mobility, and raise the DC volume resistivity [21]. In other words, the cordierite's carrier mobility is constrained, and its insulating qualities have enhanced.

Arc resistance is described as an insulating material's capacity to endure a low current, high voltage arc while resist the formation of a conducting channel over its surface. It precisely monitors the time an electrical arc can exist on the surface of an insulator before the material breaks down in seconds. All samples were examined for tolerance to arc discharges with high voltage and low current using ASTM D 495, as shown in Fig. 13. The arc on the specimen surface was ignited using two tungsten electrodes. The test was then terminated, and the resistance time was recorded in seconds. Incorporating cordierite micro particles into LSR gave outstanding arc resistance, according to the data. Arc resistance is increased at 5% cordierite filled LSR composite as 175 s, followed a decreasing trend as filler loading rose from 5 to 10%, then increasing the filler loading from 10 to 15% as 124 to 145 s by weight. Despite the fact that all of these composite samples produced results that were higher than pure LSR resistance as 23 s. Due to the cordierite filled LSR composites' increased resistance to the creation of conducting channels on the specimen's surface, these results demonstrated that the silicone system had exceptional arc resistance [22].

3.3.3 *Recovery of hydrophobicity*

Water diffusion tests were performed on both pure LSR and cordierite loaded LSR composite samples. In this test, each specimen is placed between electrodes and the test voltage is increased at a rate of roughly 1KV per second up to 12KV. The voltage must be held constant at 12KV for 1 min before being

reduced. During the test, no puncture or surface flashover occurred, and the current did not exceed 1mA throughout. All of the examined samples were recovered within 28 h and determined to be of HC1 grade. Silicone rubber with surface qualities such as anti-adhesion, low surface energy, and super hydrophobicity may limit the adhesion of solid contaminations, resulting in a "self-cleaning" surface. Thus, surface leakage currents and contamination-related pollution flashovers will be effectively suppressed [23].

3.4 Thermal properties

3.4.1 Thermal conductivity

Figure 14 depicts the influence of cordierite concentration on thermal conductivity at 55 °C mean temperature. The thermal conductivity of the filled LSR increases gradually as the cordierite loading increases up to 5 wt%; at 10 wt%, there is a minor decrease in thermal conductivity even though this value is higher than pure LSR; and again, there is an increase in thermal conductivity at the loading level of 15 wt% of cordierite. Thermal conductivity of LSR filled with 15% cordierite is 0.286 W/m K, compared to 0.252 W/m K for pure LSR. It denotes a material's ability to transport a specific amount of heat across a unit area in a unit time at a constant temperature. As a result, the higher the thermal conductivity, the greater the heat transfer rate through a unit piece of material. Polymeric insulants expand as the temperature rises. They exhibit lower thermal conductivity compared to metals/ceramics due to lower energy transfer through polymer networks. So, for HV thermal insulations, polymer insulants in foam or fibre form are widely used [24].

The high thermal conductivity fillers are spread inside the polymer and segregated from each other at low filler concentrations. The fillers' contribution to overall thermal conductivity is low, and the thermal conductivity of the composite is mostly dictated by the polymer matrix itself. With increasing filler concentrations, thermal conduction paths are produced by the creation of high-thermal-conductivity filler networks, which then considerably contribute to the composite's overall thermal conductivity [18]. In terms of thermal conductivity, the optimal filling concentration of the cordierite nano filler was discovered to be around 10% by weight.

3.4.2 TGA analysis

Thermo gravimetric analysis (TGA) of polymers is used to identify weight fluctuations as a function of time and temperature. Both decomposition and oxidation events can cause weight changes in polymeric materials. Figure 15 depicts the TG curves of cordierite loaded LSR composites. The results showed that as the temperature rose, the 5 wt% and 10 wt% cordierite composite materials demonstrated greater heat resistance than the 15 wt% cordierite, and that the 5 wt% cordierite composite performed marginally better than the 10 wt% cordierite sample in terms of minimal

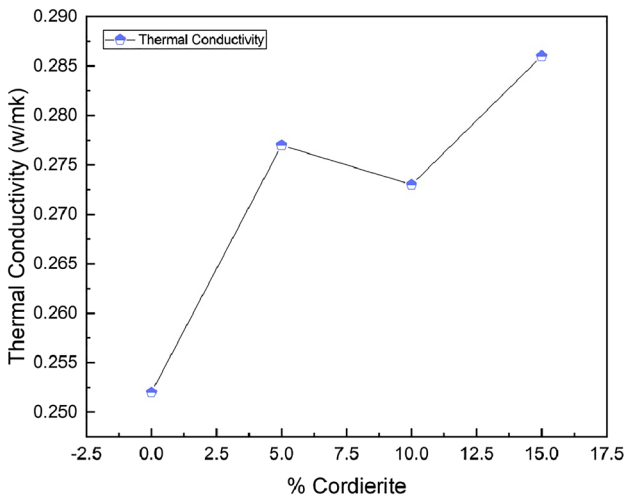

Fig. 14 Thermal conductivity of cordierite filled LSR composites at 55 °C mean temperature

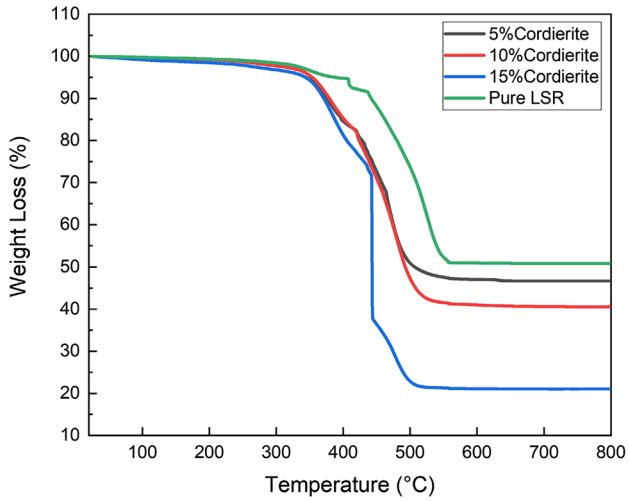

Fig. 15 Thermo gravimetric curves for the thermal degradation of pure and cordierite filled LSR composites

weight loss%, indicating greater thermal stability. This is because the phenyl pattern may impede main chain cross linking or degeneration caused mostly by oxidative breakdown of the side chains, hence boosting the thermal resistance of silicone rubber [25]. In other words, 5 wt% and 10 wt% cordierite composites have a nearly identical trend up to 500 °C. Pure LSR has a similar trend to the 5wt% cordierite sample up to 340 °C. Pure LSR has slightly stronger thermal stability above this temperature. Thermal stability decreases as filler loading percentages increase. Lower cordierite loadings are thus preferred.

The heat-resistance index (T_{HRI}), measures how well a material can withstand a heat flow. Temperature values at 5% and 30% weight loss and heat resistance index of pure LSR, pure LSR with 5 wt%, 10 wt% and 15 wt% cordierite samples displayed in Table 5 [26].

3.5 Chemical properties

Pure LSR and LSR with varied degrees of cordierite loading were submerged in 1 N salt (NaCl) and acid (HCl, and H_2SO_4) solutions. The pH of the solution and sample weights were determined every 24 h for up to 72 h before and after the samples were immersed. Figure 16 demonstrates that the weight change in the pure and composite LSR samples is negligible, and this weight change is determined by the competition between the diffusion of solution into LSR and the dissolution of filler particles and low molecular-weight siloxane in the volume of LSR into solution. Both of these processes are influenced by the temperature of the solution [8, 27]. The results reveal that the pH values of the solutions change at each interval because the ambient temperature has a significant impact on pH measurements. Water can ionise and produce a large number of hydrogen ions as the temperature rises because rising temperatures cause molecular vibrations to increase. As a result, the pH will fall. When the temperature changes, the pH of every solution varies. The difference in pH levels between temperatures is not an error. The updated pH level simply indicates the true pH of the solution at the current temperature [28].

Table 5 Temperature values at 5% and 30% weight loss and heat resistance index of pure and cordierite filled composite LSR samples

Sample name	T_5 (°C)	T_{30} (°C)	T_{HRI} (°C)
Pure LSR	387.7	509.6	225.8
LSR with 5% cordierite	352.0	457.3	203.4
LSR with 10% cordierite	353.8	452.5	200.4
LSR with 15% cordierite	343.6	442.4	197.4

4 Conclusions

In summary, the performance of the Liquid Silicone Rubber (LSR) was investigated by preparing and testing LSR composites filled with various filling concentrations (5 wt%, 10 wt%, and 15 wt%) of cordierite nano particles. After extensive research into the microstructural, mechanical, thermal, electrical, and chemical properties, conclusions can be drawn. Mechanical qualities were affected by curing time; it was discovered that the greater the curing time, larger the tensile strength and lower the curing time greater the tear strength of cordierite filled composites in order to withstand conductor load (made up of metals), wind load, and so on. Among all samples, the 48 h cured, 4 mm thick and 15 wt% cordierite filled LSR composite sample had highest tensile strength of 3.185 MPa and 24 h cured, 5 mm thick and 10 wt% cordierite filled LSR composite sample had highest tear strength of 19.045 MPa. The addition of cordierite nano filler enhanced density, DC volume resistivity, and thermal conductivity of LSR. However, the dielectric breakdown strength and arc resistance were significantly enhanced. The maximum dielectric breakdown strength was determined to be 21.72 kV/mm for a filling amount of 15% cordierite by weight and a higher value for arc resistance of 175 s is shown by 5 wt% cordierite. Furthermore, improvements were made to the hydrophobic properties. The dielectric constant was suppressed after the samples were loaded with cordierite nano particles, and low dielectric constant ratings are recommended for applications with lower electric power loss. In terms of dielectric properties, the ideal filling concentration of the cordierite nano filler was discovered to be around 5 wt% as 3.14. The chemical analysis clearly shows that the samples are not being exposed to any corrosion. Our results show that the cordierite nano particles are very effective at improving the LSR's functionality in outdoor insulation particularly in the field of transmission and distribution lines.

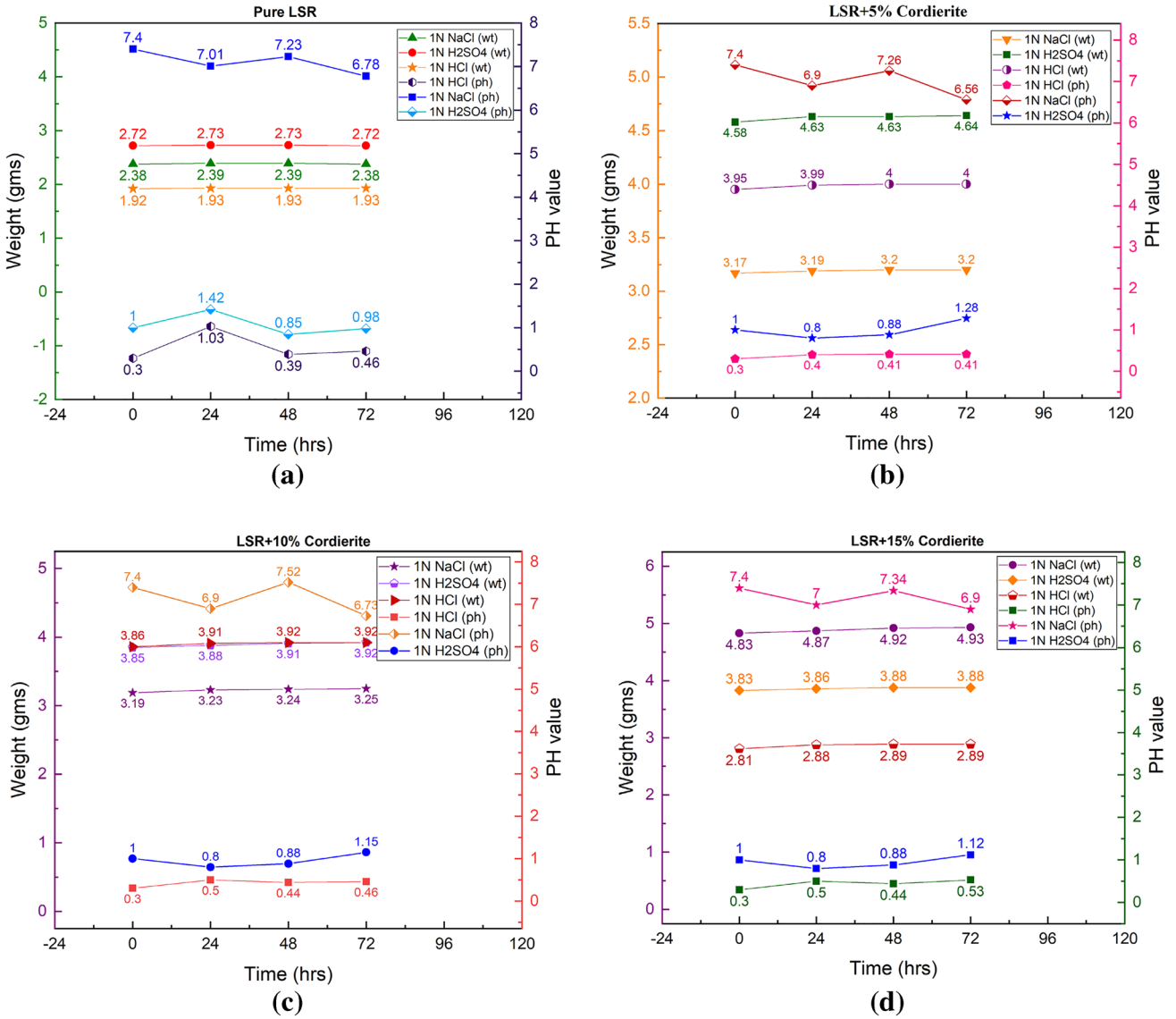

Fig. 16 Immersion of samples in NaCl, HCl, and H_2SO_4 solutions before and after 24, 48, and 72 h **a** pure LSR, **b** 5% cordierite, **c** 10% cordierite, **d** 15% cordierite filled LSR composites

Acknowledgements

We are profusely grateful to JNTU, Hyderabad for their continuous support in carrying out the research work. My thankfulness is due to the Mr. Pasupuleti Bhimudu (MD), Mr. K.K.Raju (GM), Spark insulators Pvt. Ltd., Hyderabad, India, for their whole hearted support in carrying out the part of the research work.

Author contributions

All the authors contributed equally to the manuscript at their fullest. The following contributions are listed below for the present manuscript in completion process, on behalf of all the authors corresponding author (SA) ensuring that the descriptions are accurate and approved by remaining authors.

SA: conceptualization, formal analysis, writing original draft, writing—review editing, investigation. CRA: supervision, resources, methodology. SP: supervision, resources, validation.

Funding

This research is not funded through any specific funding agencies in the public, commercial, or non-profit sectors.

Data availability

The dataset generated during and/or analyzed during the current study is available from the corresponding author on reasonable request.

Declarations

Conflict of interest The authors have no conflict either with persons or organizations/companies.

Ethical approval The ethical standards are followed in true spirit in writing this paper.

References

1. GB2093007A, United Kingdom , Anchor Hocking LLC, (1982), https://patents.google.com/patent/GB2093007A/en
2. G. Parcianello, P.E. Bernardo, P. Colombo, Cordierite ceramics from silicone resins containing nano-sized oxide particle fillers. Ceram. Int. **39**(8), 8893–8899 (2013). https://doi.org/10.1016/j.ceramint.2013.04.083
3. N.K. Singh, M.L. Verma, M. Minakshi, PEO nanocomposite polymer electrolyte for solid state symmetric capacitors. Bull. Mater. Sci. (2015). https://doi.org/10.1007/s12034-015-0980-2
4. P. Pilate, F. Delobel, Low thermal expansion ceramic and glass-ceramic materials. Encycl. Mater.: Technical Ceramics Glasses **2**, 47–58 (2021)
5. L. Li, Preparation and properties of cordierite ceramics obtained via a pouring-sintering method. Integr. Ferroelectr. **215**(1), 103–115 (2021). https://doi.org/10.1080/10584587.2021.1911230
6. S. Barua, R. Gogoi, Silicon-based nanomaterials and their polymer nanocomposites, in *Nanomaterials and Polymer Nanocomposites*. ed. by N. Karak (Elsevier, Amsterdam, 2019)
7. M. Tariq Nazir, B.T. Phung, S. Li, S. Akram, M. Ali Mehmood, G.H. Yeoh, S. Hussain, Effect of micro-nano additives on breakdown, surface tracking and mechanical performance of ethylene propylene diene monomer for high voltage insulation. J. Mater. Sci.: Mater. Electron. **30**, 14061–14071 (2019). https://doi.org/10.1007/s10854-019-01771-6
8. S. Shirisha Adupa, C.R. Pulla, Alavala, Effect of filler materials in silicone rubber for the electrical insulation applications: a review. Int. J. Appl. Eng. Res. **16**(9), 721–729 (2021). https://doi.org/10.37622/IJAER/16.9.2021.721-729
9. A. Khattak, A.U. Rehman, A. Ali, A. Mahmood, K. Imran, A. Ulasyar, H. Sheh Zad, N. Ullah, A. Khan, Multi-stressed nano and micro-silica/silicone rubber composites with improved dielectric and high-voltage insulation properties. Polymers **13**, 1400 (2021). https://doi.org/10.3390/polym13091400
10. X. Zhou, Y. Zhang, X. Shi, D. Fan, Preparation, characterization, and preliminary biocompatibility evaluation of carbon ion-implanted silicone rubber, in *Elastomers Book*. ed. by N. Cankaya (IntechOpen, London, 2017). https://doi.org/10.5772/intechopen.69251
11. M. Nadafan, R. Majid, Study of optical constants and dielectric properties of nanocrystalline α-cordierite ceramic. J. Asian. Ceam. Soc. **8**(2), 502–509 (2020). https://doi.org/10.1080/21870764.2020.1756064
12. K. Zhao, J. Li, L. Wang, D. Li, B. Liu, R. Li, X. Yu, Y. Wei, J. Liu, Z. Zhao, Preparation of cordierite monolith catalysts with the coating of K-modified spinel MnCo2O4 oxide and their catalytic performances for soot combustion. Catalysts **12**, 295 (2022). https://doi.org/10.3390/catal12030295
13. H. Khan, M. Amin, A. Ahmad, Performance evaluation of alumina trihydrate and silica-filled silicone rubber composites for outdoor high-voltage insulations. Turkish J. Electr. Eng. Comput. Sci. **26**(5), 2688–2700 (2018). https://doi.org/10.3906/elk-1609-284
14. J.-W. Zha, Z.-M. Dang, W.-K. Li, Y.-H. Zhu, Effect of micro-Si3N4-nano-Al_2O_3 co-filled particles on thermal conductivity, dielectric and mechanical properties of silicone rubber composites. IEEE Trans. Dielectr. Electr. Insul. **21**(4), 1989–1996 (2014)
15. X. Li, Z. Fang, X. Shen, Q. Yin, Z. Chen, Q. Tu, M. Pan, Study on increasing the binding amount of rubber and reinforcing filler by adding aromatic solvent oil. Polymers. **14**, 2745 (2022). https://doi.org/10.3390/polym14132745
16. Y. Ouyang, X. Li, H. Tian, L. Bai, F. Yuan, A novel branched Al2O3/silicon rubber composite with improved

thermal conductivity and excellent electrical insulation performance. Nano Mater. **11**(10), 2654 (2021). https://doi.org/10.3390/nano11102654

17. Z. Cai, X. Wang, B. Luo, W. Hong, L. Wu, L. Li, Dielectric response and breakdown behavior of polymer-ceramic nanocomposites: the effect of nanoparticle distribution. Compos. Sci. Technol. **145**, 105–113 (2017). https://doi.org/10.1016/j.compscitech.2017.03.039
18. P. Liu, L. Li, L. Wang, T. Huang, Y. Yao, W. Xu, Effects of 2D boron nitride (BN) nanoplates filler on the thermal, electrical, mechanical and dielectric properties of high temperature vulcanized silicone rubber for composite insulators. J. Alloys Compd. **774**, 396–404 (2018). https://doi.org/10.1016/j.jallcom.2018.10.002
19. H. Khan, A. Mahmood, I. Ullah, M. Amin, M.T. Nazir, Hydrophobic, dielectric and water immersion performance of 9000 h multi-stresses aged silicone rubber composites for high voltage outdoor insulation. Eng. Fail. Anal. (2021). https://doi.org/10.1016/j.engfailanal.2021.105223
20. M. Sarkarat, M. Lanagana, D. Ghosh, A. Lottes, K. Budd, R. Rajagopalan, Improved thermal conductivity and AC dielectric breakdown strength of silicone rubber/BN composites. Compos. Part C: Open Access (2020). https://doi.org/10.1016/j.jcomc.2020.100023
21. Z. Yao, J. Hu, B. Dang, J. He, Effect of different nanoparticles on tuning electrical properties of polypropylene nanocomposites. IEEE Trans. Dielectr. Electr. Insul. **24**, 3 (2017). https://doi.org/10.1109/TDEI.2017.006183
22. L. Jing, L. Ruimin, C. Chunyao, The arc resistance of binary filled silicone rubber, Annual report conference on electrical insulation and dielectric phenomena, IEEE, (2013), https://doi.org/10.1109/CEIDP.2013.6748220
23. G. Momen, M. Farzaneh, Survey of micro/nano filler use to improve silicone rubber for outdoor insulators. Rev. Adv. Mater. Sci. **27**, 1–13 (2011)
24. H. Khan, M. Amin, A. Ahmad, Characteristics of silicone composites for high voltage insulations. Rev. Adv. Mater. Sci. **56**, 91–123 (2018)
25. Y. Huang, Q. Mu, S. Zhengtao, High and low temperature resistance of phenyl silicone rubber. IOP Conf. Series: Mater. Sci. Eng. (2021). https://doi.org/10.1088/1757-899X/1048/1/012001
26. M.G. Icduygu, M. Asilturk, M. Akif, Y.K. Yalcinkaya, M. Hamidi, C. Altan, Three-dimensional nano-morphology of carbon nanotube/epoxy filled poly(methyl methacrylate). Microcapsules Mater. (2019). https://doi.org/10.3390/ma12091387
27. Z. Wang, Z.D. Jia, J.K. Jiao, Z.C. Guan, Influence of water, NaCl solution, and HNO3 solution on high-temperature vulcanized silicone rubber. IEEE Trans. Dielectr. Electr. Insul. (2016). https://doi.org/10.1109/TDEI.2015.005633
28. How Does Temperature Affect pH, Westlab Group Ltd., (2016). https://www.westlab.com/blog/2017/11/15/how-does-temperature-affect-ph